Evidence for Frustration Universality Classes in 3D Spin Glass Models [1]

Leonardo Gnesi, Roberto Petronzio, Francesco Rosati

Dipartimento di Fisica, Università degli Studi di Roma "Tor Vergata", and I.N.F.N. Sezione Roma II, via della Ricerca Scientifica, 1, I-00133 Roma, Italia

Abstract

A recently introduced Renormalization Group approach to frustrated spin models is applied in three dimensions through Monte Carlo computations. A class of spin glass models is analysed, with correlated disorder variables given by a $\mathbb{Z}_2$ gauge field. Evidence is provided for the influence of deconfinement phase transition of gauge fields on the behaviour of the associated spin models, namely in the transition from glassy to ferromagnetic behaviour. Universality classes are determined on fundamental ground by characterizing the fixed point. Moreover, the RG analysis provides good estimates of the critical temperature and the thermal index ν, with moderate computer time.

Keywords: spin glass, renormalization group, universality, frustration.
PACS Numbers: 75.10.Nr Spin-glass and other random models; 05.10.Cc Renormalization group methods.

1 Introduction

The renormalization group (RG) is an invaluable tool in the understanding of critical phenomena [1, 2]. It provides accurate estimates of critical indexes as well as a theoretical foundation of the universality principle and of the scaling theory. Many authors [8, 10, 13] have profitably used these ideas in spin glasses (SG's), even if a general RG framework for SG's was incomplete.

In a previous paper [18] a RG approach suitable for SG's has been proposed and fruitfully exploited through Monte Carlo (MC) computations in dimensions $d = 4$. A sketch of expected universality classes and the role of frustration were discussed. In the present work, these ideas has been fully developed in the more relevant and harder case of $d = 3$. The coarse graining transformation is carried out on the *overlap* field. Because of disorder average, overlap probability measure does not have the usual form $\exp(-H)$, hence it is not *a priori* clear which kind of additional interactions are generated by the RG transformation. Our proposal is to keep Hamiltonian fixed while adding gauge invariant terms to the disorder distribution, so that spins get effective correlations via correlations of gauge fields. Asymptotic decrease regimes of Wilson loops in pure gauge model [6], namely the *weak* and *strong* decrease, can induce very different behaviour on related spin systems. In the former case, frustration effects are very small locally and increase weakly at long range: spins prefer to order ferromagnetically. In the case of strong decrease, instead, average Wilson loop rapidly fall to zero and a SG behaviour is expected. The existence of two fixed points corresponding to the above mentioned universality classes is supported by evidence from our analysis. Moreover, our estimates of critical temperature $T_{\rm c}$ and thermal index ν are in good agreement with previous results [14, 17]. Notice that a less frustrated system gets ordered more easily, giving rise to higher critical temperatures. This property can be exploited to perform Monte Carlo computations of SG models at very low $T/T_{\rm c}$ ratios [19].

[1] This work is supported in part by "Enrico Fermi Research Center", via Panisperna 89, Rome.

Numerical methods based on Monte Carlo simulations of SG's are particularly hard in $d = 3$ basically because of the low temperatures involved. This requires very long Monte Carlo runs to reach ergodic regime. Parallel Tempering (PT) algorithm, which we implement, is adequate to face this kind of problems but unfortunately it hides the meaning of MC autocorrelation time, making standard error estimates not efficient. Aiming to control both ergodicity and MC-errors, we employ a method based on the analysis of MC-PT dynamics, which turns out to be quantitative and more stringent than usual PT efficiency checks.

2 The spin glass model and the overlap field

Let σ_x be Ising spins located at the sites of a d-dimensional cubic lattice Λ, with L points on each side ($x \in \Lambda \subset \mathbb{Z}^d$ with toroidal topology, *i.e.*, periodic boundary conditions are assumed). The typical spin glass model of Edwards and Anderson [4] is defined by two prescriptions: 1. The spins are distributed according to the Boltzmann weight given by the following Hamiltonian

$$H(J,\, \sigma) = -\sum_{\langle x,\, y\rangle} J_{xy}\sigma_x\sigma_y; \tag{1}$$

2. The quenched disordered interactions J_{xy} are random variables, with a given distribution. The sum in (1) is over pairs of neighboring sites in Λ. We will denote by E the expectation on J variables, and define

$$E(J_{xy}) = 0, \;\; E(J_{xy}^2) = 1. \tag{2}$$

The Boltzmann–Gibbs measure on the spin variables will be denoted by angular brackets $\langle\cdot\rangle$. Averages over the disorder are taken only after Boltzmann averages are calculated, and the thermodynamic limit for the appropriate quantities is eventually taken afterwords. A generic observable can be expressed in terms of correlations *of* correlation functions,

$$E\left[\langle f_1(\sigma)\rangle \dots \langle f_s(\sigma)\rangle\right], \tag{3}$$

where f_i, $i = 1, \dots, s$ are functions of the spin field. Consider the following gauge symmetry of the Hamiltonian,

$$\begin{cases} J_{xy} \to J'_{xy} = \varepsilon_x J_{xy}\varepsilon_y \\ \sigma_x \to \sigma'_x = \varepsilon_x\sigma_x \end{cases} \tag{4}$$

where $\varepsilon_x = \pm 1$ are the gauge group parameters. If the distribution of the J's is gauge-invariant, the model, characterized by observables (3), is also gauge-symmetric. This happens, for instance, in the traditional case of even, independent, identically distributed J variables (E-A model).

A central concept is the overlap field. Consider s replicas (copies) of the spin variables $\sigma^{(a)}$, $a = 1, \dots, s$. The Hamiltonian of the replicated system is given by $\mathcal{H} = \sum_a H(J,\, \sigma^{(a)})$: replicas are independent from each other, but feel the *same* disorder configuration J. For any pair of replicas $(a, b),\ 1 \le a < b \le s$, define the *overlap field*, $q_x^{(a,b)}$,

$$q_x^{(a,b)} = \sigma_x^{(a)}\sigma_x^{(b)} \;\in \mathbb{Z}_2. \tag{5}$$

The probability distribution of the overlap fields, μ, can be implicitly defined through the overlap expectations, that involve both the thermal average and the average E over disorder. For any smooth function F define

$$\left\langle\!\!\left\langle F\left(q_x^{(12)}, q_y^{(23)}, \dots\right)\right\rangle\!\!\right\rangle = E\left[\left\langle F\left(\sigma_x^{(1)}\sigma_x^{(2)},\, \sigma_y^{(2)}\sigma_y^{(3)}, \dots\right)\right\rangle\right], \tag{6}$$

where expectation with respect to the μ distribution is denoted by $\langle\!\langle\cdot\rangle\!\rangle$. All physical observables can be expressed in terms of overlap observables, so that the full physical meaning of these models is contained in the overlap probability measure.

Let us introduce the volume average of the overlap field, the total overlap, often simply referred to as "overlap",

$$q^{(a,b)} = \frac{1}{|\Lambda|} \sum_x q_x^{(a,b)}. \tag{7}$$

For two replicas, the distribution of the overlap $q^{(1,2)}$ will be denoted by $P^{(2)}$. An other interesting observable is the two points, connected correlation function of the overlap field:

$$C(r) = \frac{1}{|\Lambda|} \sum_x \langle\!\langle q_x^{(1,2)} q_{x+r}^{(1,2)} \rangle\!\rangle_c, \tag{8}$$

3 A renormalization group for spin glass models

The total overlap is the order parameter of the model. In the high temperature phase, including the critical point, it should be zero in the infinite volume limit, while in the low temperature phase it is expected to fluctuate [7, 9, 10]. Therefore, the critical point can be characterized by a divergence of the correlation length associated to (8). For this reason, it is natural to define the RG transformation on the overlap field. In the following we consider only two replicas, and omit the replica indexes on the overlap variables.

Let $B_x^n \subset \Lambda$ be the cube of size n located in x and $\Lambda_n \subset \mathbb{Z}^d$ a cubic lattice of side L/n. Because of $\mathbb{Z}_2$ symmetry, the coarse grained field $q'_{x'}$ can be defined [8] on Λ_n as the sign of the majority of overlaps inside a block centered on $x = nx'$. The renormalization group transformation for a rescaling factor n then acts on the overlap distribution μ as follows:

$$\mu'_n(q') = \sum_{\{q\}} \mu(q) \prod_{x' \in \Lambda_n} \delta\left(q'_{x'}, \mathrm{sign}\left(\sum_{y \in B^n_{nx'}} q_y \right) \right), \tag{9}$$

where the sum on the r.h.s. runs over all the $2^{|\Lambda|}$ configurations of overlaps q_x and $\delta(a,\, b)$ is 1 for $a = b$ and zero otherwise. For $m = n^k$, one defines the distribution $\mu_n^{(k)}(q^{(k)})$ as the result of k iterations of (9), and the semi-group property holds by construction.

Extending these definitions, in the appropriate way, to the thermodynamic limit, the transformation may be iterated indefinitely and eventually a non-trivial asymptotic distribution μ^* may be reached. However, to carry out useful RG calculations an approximation scheme must be chosen. In this work we have used the Monte Carlo approach, for which the main approximation is the use of a finite lattice. The basic effect is that of neglecting the influence of distant regions of the lattice on each other in the calculation of $\mu'_n(q')$ from $\mu(q)$ [3]. Indeed, a fundamental property of a RG transformation is that the parameters representing the renormalized distribution must depend analytically on the unrenormalized parameters. One assumes that the dependence of μ'_n on μ is analytic, because local observables of q' in one region of the lattice are not appreciably affected by distant regions of the system, in spite of the eventually infinite correlation length. For the very same reason, the computation of local observables of the field q' should be weakly affected by finite lattice effects, on the contrary of what happens to observables of the unrenormalized field q.

On a finite lattice the transformation (9) may be limited to a very small number of iterations. Another typical problem is the truncation error due to the projection of renormalized distributions onto a space with a restricted number of couplings. To minimize the effects of these approximations, a different RG scheme [11, 18] has been adopted. We define the renormalized fields q'_x on Λ_n as given just by the transformation (9) with $n = L/\ell$ (with small typical values, *e.g.* $\ell = 2, 3$); the renormalized distribution will be denoted by $\mu'(q')$. Notice that, with only one iteration, Λ_n is a lattice with volume ℓ^3. Due to the smallness of Λ_n only a few couplings are allowed and there is no truncation error. The procedure is repeated for different values L, L' and the ratio L/L' is interpreted as a scaling factor [11] (but see also [12]). Moreover, the sequence will give better results for increasing n, because the group parameter will be large and, at the same time, the size of the initial system will be affected by smaller finite-size effects. Given the large size of blocks, we also expect the results to be not dramatically dependent on the choice of blocking transformation.

The RG transformation is naturally defined on the probability distribution of the overlap field. For the purpose of calculations this distribution is well characterized by the expectations of a set of (translation-invariant) observables. It is the approach that has been followed in this work. However, the question may be raised of how to express such a distribution in terms of physically meaningful parameters. It is clear that the traditional exponential form, $\exp(-H)$, has no physical relevance, due to the involved definition of the overlap field distribution in the original model. To state the question in a different way: which additional interactions between the microscopic variables are generated as a result of the RG transformation ? The answer to this question is important in order to get high precision estimates of the critical indexes, through the observation of the effects of irrelevant perturbations to the fixed point. We propose the following parameterization, that proved to be effective in the case of dimension $d = 4$ [18]. The Hamiltonian, given by (1), is kept fixed, while the disorder is distributed according to a general gauge action:

$$\rho_K(J) = \exp\left(\sum\nolimits_i K_i\, W_i(J)\right), \tag{10}$$

where the $K_i \in \mathbb{R}$ are parameters and the W_i's are Wilson's loops, *i.e.*, products of J's along closed paths. Let us stress that the effects of this parameterization are that spins get non trivial extra correlations through the "dressing" of interactions. The resulting set of spin models will be discussed in more detail in next section of this paper.

4 Spin models with quenched gauge-field interactions

Consider the E-A spin Hamiltonian (1), and assume the quenched interactions are distributed according to a general, gauge-invariant distribution function such as (10). A fairly large set of models may be defined in this way. For the sake of simplicity, let us restrict our attention to the disorder distributions of the following form,

$$\rho_K(J) = C_K\, \exp\left(K_1 \sum_{\langle x,\, y\rangle} J_{xy}^2 + K_2 \sum_{\langle x,\, y\rangle} J_{xy}^4 + K_3 \sum_{\alpha} \Box_\alpha\right), \tag{11}$$

where $C_K \in \mathbb{R}$ is a normalization constant, and the symbol $\Box$ denotes the plaquette terms of the kind $J_{x,y}J_{y,z}J_{z,w}J_{w,x}$. Expectation with respect to this distribution will be denoted by E_K. We notice that the Gaussian Edwards-Anderson model corresponds to $K_1 = -1/2,\ K_2 = K_3 = 0$, while the $\mathbb{Z}_2$, E-A model is obtained in the limit $K_1, K_2 \to \infty,\ \text{s.t. } K_1/K_2 = -2,\ K_3 = 0$. But a more interesting model is obtained by adding a plaquette term (*i.e.*, $K_3 \neq 0$):

$$\rho_K(J) = C_K\, e^{K_3 \sum_\alpha \Box_\alpha},\ \ J \in \mathbb{Z}_2^{d|\Lambda|}, \tag{12}$$

Considering the disorder variables only, this is the well known pure gauge $\mathbb{Z}_2$ model [5]. The partition function, the free energy and the internal energy density are defined by

$$Z_\Lambda(K_3) = \sum\nolimits_{\{J_{xy}=\pm 1\}} \exp\left(K_3 \sum\nolimits_\alpha \Box_\alpha\right) = e^{-K_3 F_\Lambda(K_3)} \tag{13}$$

$$u_\Lambda(K_3) = -E_{K_3}\left(\sum\nolimits_\alpha \Box_\alpha / N_\Box\right). \tag{14}$$

The energy density u_Λ is equal to minus the average plaquette, thus it gives a measure of the short – range frustration of the spin system.

Let us denote by w_γ the product of the J's along a closed path γ,

$$w_\gamma = \prod_\gamma J_{xy} = \prod_{\alpha \in S} \Box_\alpha, \tag{15}$$

where S is a surface bounded by γ. Two canonical asymptotic regimes may be distinguished: a *weak decrease* regime, characterized by $E(w_\gamma) \approx e^{-L}$; a *strong decrease* regime, where $E(w_\gamma) \approx e^{-A}$. L and A denote the perimeter of γ and the area of the surface S. In various models a transition from the strong to

the weak decrease is observed as the average plaquette increases. The model (12), in 3 dimensions, exhibits a second order phase transition at $K_3 = K_3^c \simeq 0.7613$. The corresponding order parameter is the square Polyakov loop, $p^2 = (p_1^2 + p_2^2 + p_3^2)/3$, where p_i is the average Wilson loop along a path that closes itself exploiting the periodicity of the b.c.'s in direction i. The quantity $E(w_\gamma)$ is relevant for the spin system associated to the gauge field [6], as it is related to the average frustration on the range γ.

We are now in the position to sketch the behavior of the spin system corresponding to the pure-gauge disorder distribution (12) [18]:

$K_3 \to \infty$ The disorder is in a ground state of the gauge Hamiltonian, characterized by $E_{K_3}(\Box) = 1$, $p_i = \pm 1$. Up to a gauge transformation, the spin model is an Ising model, with periodic b.c. in the directions i for which $p_i = 1$ and anti-periodic in the others.

$K^c < K_3 < +\infty$ The disorder is in the weak decrease phase: frustration effects are very small locally ($E_{K_3}(\Box) \approx 1$) and increase weakly at long range. The spin system is expected to be ferromagnetic.

$-K^c < K_3 < K^c$ The disorder is in the strong decrease phase. The average plaquette is approximated by $E_{K_3}(\Box) \approx K_3$, except in the region very close to the transition. However, frustration moves rapidly toward $1/2$ for increasing range. Spin glass behavior is expected.

$K_3 \to -\infty$ The gauge field is in a "fully frustrated" configuration, *i.e.*, all plaquettes are frustrated.

The behavior in the region $-\infty < K_3 < K^c$ is still an open question.

These different qualitative regimes should correspond to different universality classes of the spin system. Exploiting the RG approach introduced in the previous section, we will be able to characterize the universality classes in terms of different fixed points.

5 Analysis of Monte Carlo computations

The Renormalization Group analysis described in section 3 was performed numerically by dynamic Monte Carlo computations. We employed Hamiltonian (1) in dimension $d = 3$, with periodic boundary conditions and $\mathbb{Z}_2$ quenched disorder distributed according (12). Besides the traditional Edwards-Anderson model, corresponding to the case $K_3 = 0$, we simulated two other models, with $K_3 = 0.3$ and 0.8, in order to verify the conjecture on universality classes made in section 4. Moreover, the MC-RG analysis was performed on the Ising model, corresponding to $K_3 = \infty$, as a test of the method, and for a comparison to the other models.

The choice of K_3 values deserves some comments. $K_3 = 0.3$ is far from the critical value $K_3^c \simeq 0.7613$ to avoid cross-over effects, and is quite different from the E-A model: frustration is $f_{0.3} \simeq 0.35$, compared to $f_0 = 0.5$. In the deconfined phase, $K_3 = 0.8$ gives a very low frustration $f_{0.8} \simeq 0.015$. Lower values of K_3 provide slightly higher frustration, but we considered unwise a value too close to K_3^c, even though the critical coupling is lower in a finite lattice. Nevertheless, the model is quite different from the Ising model, as is shown, for instance, by the value of the square Polyakov loop, $p^2 \simeq 0.65$. Among the eight possible pure phases, we chose the one characterized by positive Polyakov loops, *i.e.*, $p_i \geq 0$.

For each model, a quite large number of samples (with different configurations of the disorder J) were simulated, as reported in table 1. The required disorder configurations were generated by an independent MC process on the gauge fields, according to distribution (12). This step is quite simple with nowadays computers. The average correlation between J configurations is never greater than 10^{-4}.

The MC runs on the spin variables are more complicated. We simulated lattices of linear size $L = 8, 12, 16$ for all models, together with additional $L = 24$ for models $K_3 = 0.8$ and Ising and $L = 10, 14$ for $K_3 = 0$ whose significance will be clear later. The code makes use of Parallel Tempering (PT) algorithm and multi-spin encoding. For every Metropolis update, a PT step was performed. Two replicas were simulated through independent MC chains in order to compute overlap observables. The RG transformation was carried out following the procedure explained in section 3 [11]. Therefore, the

RG parameter n takes the values 4, 6 and 8 (and 12) as well as 5, 7 for $L = 10,\ 14$. To characterize the distribution μ', we measured the following observables of the random field q':

$$A_1 = \frac{1}{3|\Lambda'|} \sum_{x,l:|l|=1} \langle\!\langle q'_x q'_{x+l} \rangle\!\rangle \qquad A_4 = \langle\!\langle S^2 \rangle\!\rangle \tag{16}$$

$$A_2 = \frac{1}{3|\Lambda'|} \sum_{x,l:|l|=\sqrt{2}} \langle\!\langle q'_x q'_{x+l} \rangle\!\rangle \qquad A_5 = \langle\!\langle S^4 \rangle\!\rangle \tag{17}$$

$$A_3 = \frac{1}{3|\Lambda'|} {\sum_{x,y,z,w}}' \langle\!\langle q'_x q'_y q'_z q'_w \rangle\!\rangle \qquad A_6 = \langle\!\langle (0.4 + S^2)^{-1} \rangle\!\rangle \tag{18}$$

where $S = |\Lambda'|^{-1} \sum_x q'_x$, and the sum in A_3 runs over the 4-uples of sites located on plaquettes. Notice that observable A_6 is sensible to the small values of S, as opposed to A_4 and A_5, and 0.4 is an arbitrary cut-off. For the sign function involved in the definition of q', a tie-breaker was used in the undetermined zero cases. Models with $L = 10,\ 14$ are unaffected by this procedure and, in principle, this difference in the transformation rule could provide different results. Moreover, we have explicitly measured the β derivative of each observable, computing the connected correlation function with the Hamiltonian. In the definition of the blocks, the choice of the origin is arbitrary. In order to improve the quality of statistics, we choose to average the measures over eight different origins. The lower simulated temperature, $T_{\min}$ in Table 1, was chosen around $0.9T_{\rm c}$, according to previous estimates of $T_{\rm c}$, for the $K_3 = 0$ model. The efficiency of the PT algorithm was checked through the acceptance rate of temperature swaps. We ensured it was roughly 1/2 in the most difficult runs, and never below 40%.

In the rest of this section we discuss the checks on ergodicity of MC runs and error estimates. Generally speaking, as higher values of K_3 correspond to lower frustration, systems should get ordered more easily so that we expect critical temperatures to increase with K_3, carrying on a global improvement of MC-PT performances. On the opposite, negative values of K_3 presumably give rise to very low critical temperatures thus making simulations very difficult, at least in dimension $d = 3$. A well known problem in performing Monte Carlo computations on glassy systems is the difficulty in reaching ergodic regime, due to strong metastability effects and to the large number of nearly degenerate ground states. A very powerful — albeit indirect — criterion to ensure ergodicity makes use of the observation of (Monte Carlo) time spent by the system at each temperature of the PT set. This must be approximately the same for each temperature. We measured the ratio r of the time spent in the most visited T over the less visited one. The histograms of the results are presented in Table 1.

Ergodicity may be verified explicitly by analyzing the time sequence of the measures. By the same token we can estimate the statistical error of the measures taken on a single sample. The algorithm employed measures observables at each MC-PT step. These measures were averaged in groups of 1024, providing a set of a few hundred points per sample and per temperature. One problem of PT algorithm is that of properly defining an autocorrelation time. However, these points may be considered reasonably independent from each other. Thus, we can estimate the statistical error on a single sample. Then the procedure is repeated: the measures are averaged over groups of points, obtaining a different estimate of the error. Clearly, as the size of the groups increases, the resulting points will be less correlated producing a better (usually larger) estimate of the error. In Figure 1 (left), we plotted the histogram of the single-sample relative errors on observable A_2, in our worst-case simulation ($K_3 = 0,\ L = 16,\ T = 1.02$). The quantity l denotes the number of initial points and a is the number of groups so that the size of groups is roughly l/a. The results seem to be very stable in a.

We can check ergodicity in a similar way. On each group $i = 1, \ldots, a$ we compute, along with the average observable $x_i^{(a)}$, the error on the average, *i.e.*, its standard deviation (denoted by $\tau_i^{(a)}$). If ergodicity is reached on a time scale l/a then the $x_i^{(a)}$'s will be nearly aligned and fluctuations around the mean will be of order $\sim \bar\tau = a^{-1} \sum_i \tau_i^{(a)}$. On the other hand, if l/a is a too short time scale, the points will spread with very large fluctuations around the mean. Let us denote by σ_a the standard deviation of group averages $x_i^{(a)}$. To characterize ergodicity we thus measure the ratio $\eta = \sigma_a/\bar\tau$, expecting $\eta \lesssim 1$ when ergodicity is

K_3	L	$N_{\rm MC}/10^5$	$N_{\rm S}$	N_β	$T_{\rm min}$	$T_{\rm max}$	$r \geq \sqrt{2}$	$r \geq 2$	$r \geq 4$
0	8	1.0	36096	16	1.00	2.30	0	0	0
	10	1.2	10240	19	1.00	2.35	0.02	0	0
	12	1.6	15936	27	1.00	2.30	0.18	0.005	0
	14	2.0	5632	30	1.01	2.32	0.38	0.04	0
	16	2.4	3328	33	1.02	2.30	0.50	0.09	0.001
0.3	8	1.0	20160	26	1.20	3.00	0	0	0
	12	1.0	9216	36	1.10	2.85	0.55	0.12	0.005
	16	2.0	2880	45	1.20	2.96	0.84	0.40	0.08
0.8	8	0.5	4000	11	4.00	5.00	0	0	0
	12	0.2	4000	20	4.05	5.00	0	0	0
	16	0.5	512	28	3.92	5.00	0.37	0.02	0
	24	0.5	512	9	4.44	4.52	0	0	0

Table 1: *Parameters of MC-PT runs. The same number of MC-PT steps, $N_{\rm MC-PT}$, was used for thermalization and measurements. We report also the number of different disorder samples $N_{\rm S}$, the total number of temperatures N_β (together with minimum and maximum values) for the PT algorithm, and the histograms on visiting frequencies.*

reached, and $\eta \gg 1$ when is not. The histograms of the results for different samples are shown in Figure 1 (right). Let us underline that the results should be extrapolated to $a = 1$: a "good" MC run should not be much longer than necessary.

From general arguments, the total statistical error on observable A, ΔA, can be estimated as follows:

$$(\Delta A)^2 = \frac{\epsilon_S^2 + \sigma^2}{N_S} \tag{19}$$

where ϵ_S^2 is the sample-to-sample variance, $N_{\rm S}$ the total number of simulated samples and σ is the single-sample error. As typical sample-to-sample fluctuations of observables are of order 100%, the single-sample errors can be neglected.

6 Numerical results

Performing the Renormalization Group analysis explained in section 3, we are able to characterize universality classes depending on frustration parameter, pointing out the influence of deconfinement phase transition of gauge fields on the behavior of the associated spin model, namely in the transition from glassy to ferromagnetic behavior. In particular the results confirm the conjecture [6] that the asymptotic regime of long range frustration is responsible for the glassy behaviour. Universality classes were determined by characterizing the fixed point, therefore on fundamental grounds, without relying on phenomenological comparison of critical indexes. Moreover, the RG analysis provided good estimates of the critical temperature, T_c, and thermal index ν, of the four models considered: $K_3 = 0,\, 0.3,\, 0.8$ and Ising. As we will show in this section, the fundamental determination of universality classes allows to consider ν_0 and $\nu_{0.3}$ as *independent estimates* of the thermal index of the glassy fixed point.

In order to damp irrelevant perturbations, and to enhance the effect of the relevant coupling [11], we chose to employ the largest possible values of $n = L/L' = 4,\, 6,\, 8,\, (12)$, thus setting the renormalized lattice size equal to $L' = 2$. As a drawback, observables $A_1, \ldots, A_6$ turned out to be strongly correlated, making it impossible to perform a full linearization of the RG transformation on the fixed point and to estimate irrelevant exponents.

Observables defined on different lattices characterize the trajectory of RG flow and, at the critical temperature, they move toward a fixed point where they become independent of the initial lattice. As a

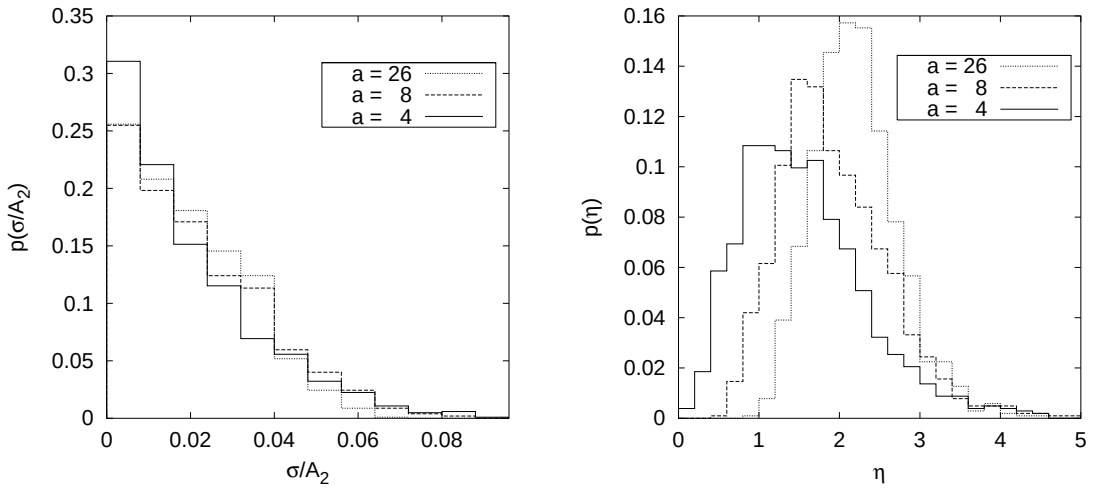

Figure 1: *Relative error (on the left) and ergodicity distribution (right) of observable A_2 on various time scales l/a in the E-A model $K_3 = 0,\ L = 16,\ T = 1.02$. The total number of samples examined is 1024. Relative error diagram is quite stable and more than 99% of sample have relative errors lower than 0.08, on all time scales. On the right, the distribution of η shows that on short time scales ($a = 26$), 63% of samples have $\eta > 2$; this number drops to 41% for $a = 8$, and to 25% for $a = 4$, indicating run length is essentially correct. Single sample errors and ergodicity both improve at higher temperatures.*

function of temperature, observables will cross in a point which can be estimated as the critical temperature T_c. The linearization around the crossing point of two quantities $A(L_1)$ and $A(L_2)$ determines the thermal exponent through:

$$\nu^{-1}(A) = \frac{\ln\left[\frac{dA(L_1)}{d\beta}|_{\beta_c} \ / \ \frac{dA(L_2)}{d\beta}|_{\beta_c}\right]}{\ln(L_1/L_2)} \tag{20}$$

where $\beta^{-1} = T$ and derivatives are computed at the critical point. In Figures 2 and 3 is plotted observable A_1 as a function of temperature, the points size being larger than the error bars, except in the detail of Figure 2. In accordance with [14], Figure 2 seems to rule out a Kosterlitz-Thouless transition type, for in that case the curves should merge under T_c. Moreover, the resulting estimates of ν obtained with formula (20) are the best proof that curves cross with different slopes.

Data, for each A_i, were fitted to allow for extrapolation to the critical point. We notice incidentally that the measures of derivatives with respect to β greatly improved the precision of the results. The errors on T_c and ν were estimated with the following procedure: measures taken on different samples were grouped in 32 blocks and averaged over 31 blocks to compute the results. The procedure was repeated with different blocks, obtaining 32 different estimates of T_c and ν. Then, errors were estimated with jackknife formula.

The results shown in Table 2 were averaged over the six observables. Notice that, for glassy models, only two of the three estimates provided are independent, as they all come from the same three lattices. The error on T_c and, as a consequence, on ν is larger for the pair $(16,\ 12)$ because of the very close slopes of curves. A transient effect due to the flow of irrelevant couplings seems to be present, but cannot be measured within current precision and lattice sizes. Results for $K_3 = 0.8$ have much higher precision, revealing that sample-to-sample fluctuations are very small. The analysis of the Ising model was performed to serve as a benchmark of the method. Recent high precision estimates, in the infinite volume limit, are as follows [15, 17]: $T_c = 4.511524(2),\ \nu = 0.63012(16)$. The results for $K_3 = 0.8$ and Ising confirm the effectiveness of the method, and suggest that the evaluation of irrelevant exponents is necessary in order for to obtain reliable results at higher precision. Notice the results from lattices $(14,\ 10)$: in this case a different transformation Θ was used (the tie-breaker is not necessary). Our results for the Edwards-Anderson model are in agreement with previous estimates [13, 14], obtained with finite-size scaling techniques on much

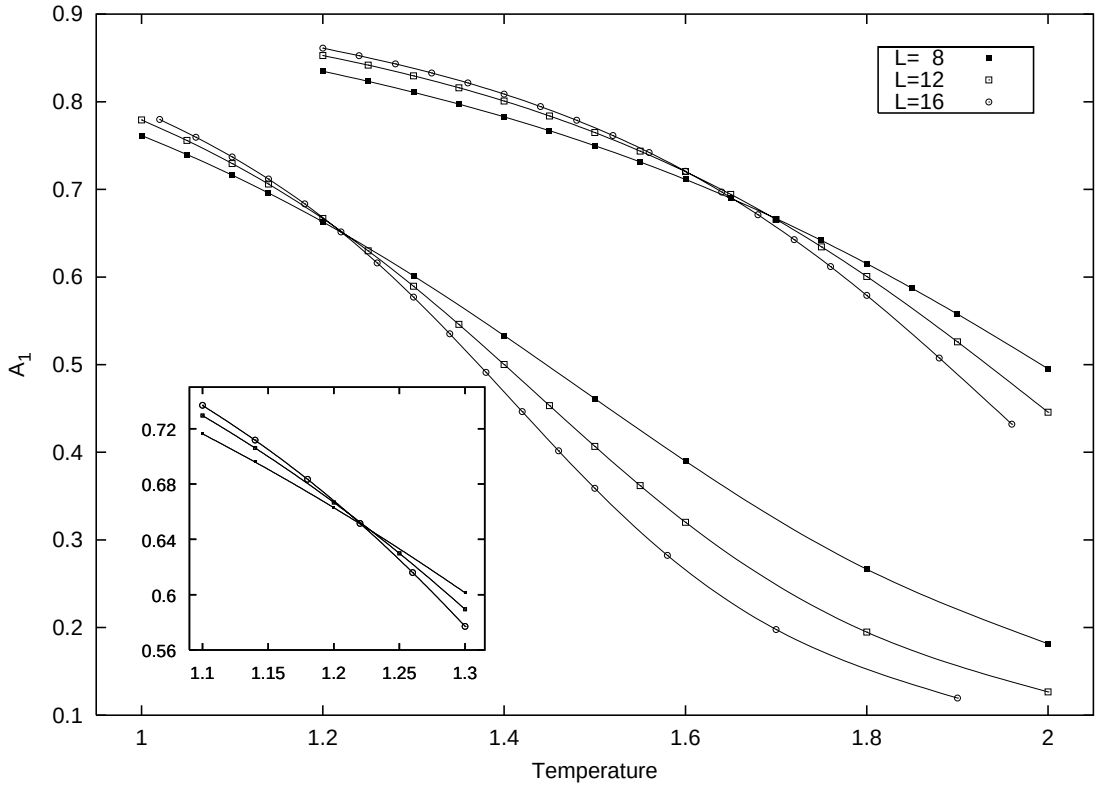

Figure 2: *Observable A_1 versus temperature for E-A model $K_3 = 0$ (on bottom, with a magnified detail) and for model $K_3 = 0.3$ (top). Points size is larger than error-bars, except in the detail.*

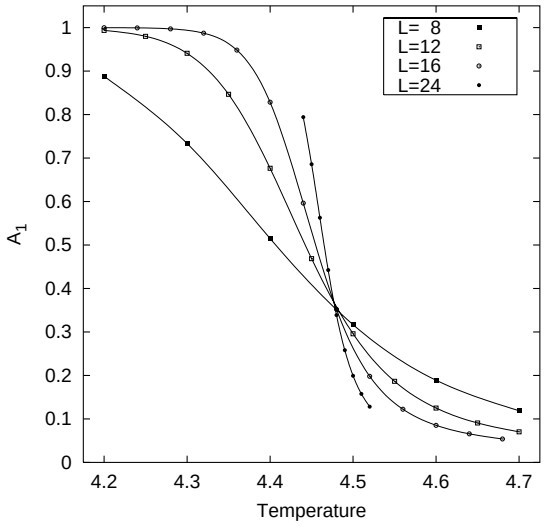

Figure 3: *Observable A_1 versus temperature for $K_3 = 0.8$.*

K_3	$(L_2,\, L_1)$	$T_{\rm c}$	ν
0	(12, 8)	1.225 (10)	1.89 (9)
	(16, 8)	1.221 (12)	1.96 (12)
	(16, 12)	1.215 (25)	2.11 (34)
0	(14, 10)	1.186 (36)	2.12 (36)
0.3	(12, 8)	1.732 (25)	1.87 (13)
	(16, 8)	1.681 (20)	1.87 (11)
	(16, 12)	1.62 (6)	1.9 (5)
0.8	(12, 8)	4.4833 (6)	0.6637 (8)
	(16, 8)	4.4793 (6)	0.6563 (10)
	(16, 12)	4.4761 (13)	0.652 (3)
	(24, 8)	4.4779 (2)	0.6512 (3)
	(24, 12)	4.4767 (3)	0.6439 (5)
	(24, 16)	4.4769 (7)	0.6395 (12)
∞	(12, 8)	4.5213 (2)	0.6588 (9)
	(16, 8)	4.5178 (1)	0.6537 (7)
	(16, 12)	4.5149 (2)	0.648 (2)
	(24, 8)	4.5149 (1)	0.6495 (5)
	(24, 12)	4.5134 (1)	0.6441 (8)
	(24, 16)	4.5128 (1)	0.6417 (14)

Table 2: *Estimates of the critical temperature ($T_{\rm c}$) and the critical index ν. $K_3 = \infty$ denotes the Ising model (with periodic b. c.).*

larger lattices and exploiting dedicated machines or supercomputers.

Finally, we present in Table 3 the values of observables $A_1, \ldots, A_6$ at the estimated critical point. These data roughly characterize the fixed point on the lattice $L' = 2$. Remnant effects of irrelevant couplings affect the determination of T_c, and therefore our extrapolation. Nevertheless, data points clearly point out the existence of different universality classes below and above the deconfinement transition. Within current precision, we can very well assume that model $K_3 = 0,\, 0.3$ are in the same *spin glass* universality class, while $K_3 = 0.8$ appears to be in the same class as Ising model.

7 Conclusions

A recently introduced [18] (see however [8]) Renormalization Group transformation suitable for disordered spin models is explained in detail and applied numerically in the three dimensional case. Universality classes depending on a frustration parameter have been characterized, pointing out the influence of deconfinement phase transition of gauge fields on the behaviour of the associated spin model, namely in the transition from glassy to ferromagnetic behavior. The study of universality classes relies on the direct detection of fixed points, therefore on fundamental grounds, without relying on phenomenological comparison of critical indexes. Moreover, the RG analysis provided good estimates of the critical temperature, T_c, and thermal index ν, of the four models considered: $K_3 = 0,\, 0.3,\, 0.8$ and Ising. As we have shown, the fundamental determination of universality classes allows to consider ν_0 and $\nu_{0.3}$ as *independent estimates* of the thermal index of the glassy fixed point. These results are in agreement with previous numerical estimates on the Edwards-Anderson model, obtained exploiting Finite-Size Scaling Ansatz [13, 14, 16]. For the small lattices and the reasonable computer time employed, this RG technique is to be considered very effective in order to compute critical properties of disordered systems.

K_3	$(L_1,\, L_2)$	A_1	A_2	A_3	A_4	A_5	A_6
0	$(12,\, 8)$	0.647 (6)	0.580 (8)	0.520 (7)	0.653 (7)	0.570 (8)	1.143 (10)
	$(16,\, 8)$	0.650 (7)	0.583 (9)	0.523 (8)	0.656 (8)	0.573 (9)	1.139 (11)
	$(16,\, 12)$	0.656 (18)	0.589 (23)	0.528 (20)	0.660 (19)	0.578 (21)	1.133 (27)
0.3	$(12,\, 8)$	0.645 (14)	0.574 (17)	0.512 (16)	0.649 (14)	0.562 (15)	1.145 (20)
	$(16,\, 8)$	0.670 (10)	0.603 (12)	0.543 (12)	0.673 (10)	0.592 (11)	1.114 (14)
	$(16,\, 12)$	0.71 (3)	0.65 (4)	0.59 (4)	0.71 (3)	0.64 (4)	1.07 (4)
0.8	$(12,\, 8)$	0.3429 (14)	0.2920 (15)	0.1840 (11)	0.3969 (13)	0.2805 (13)	1.5103 (21)
	$(16,\, 8)$	0.3505 (12)	0.2990 (13)	0.1924 (11)	0.4032 (11)	0.2877 (11)	1.5012 (19)
	$(16,\, 12)$	0.369 (5)	0.316 (5)	0.213 (4)	0.419 (4)	0.305 (5)	1.479 (7)
	$(24,\, 16)$	0.367 (6)	0.310 (6)	0.215 (5)	0.415 (5)	0.303 (5)	1.489 (9)
∞	$(12,\, 8)$	0.3390 (4)	0.2881 (4)	0.1830 (3)	0.3936 (4)	0.2780 (4)	1.5166 (6)
	$(16,\, 8)$	0.3460 (3)	0.2945 (4)	0.1899 (3)	0.3993 (3)	0.2842 (3)	1.5078 (5)
	$(16,\, 12)$	0.3629 (6)	0.3099 (8)	0.2068 (6)	0.4133 (6)	0.2994 (6)	1.4869 (11)
	$(24,\, 16)$	0.3757 (8)	0.3207 (9)	0.2202 (7)	0.4234 (8)	0.3108 (8)	1.4726 (12)

Table 3: *Characterization of the fixed points: observables $A_1, \ldots, A_6$ computed on the lattice L_2 at the estimated critical temperature $T_c(L_1,\, L_2)$.*

Acknowledgments

The authors wish to warmly thank Giorgio Parisi for interesting discussions.

References

[1] G. Jona-Lasinio, cond-mat/0009219, (2000)

[2] K. G. Wilson, Phys. Rev. B **4**, (1971) 3174; K. G. Wilson, Phys. Rev. B **4**, (1971) 3184.

[3] T. L. Bell and K. G. Wilson, Phys. Rev. B **11**, (1975) 3431.

[4] S. F. Edwards and P. W. Anderson, J. Phys. F **5**, (1975) 965–974.

[5] R. Balian, J. M. Drouffe and C. Itzykson, Phys. Rev. D **11**, (1975) 2098.

[6] G. Toulouse, Comm. Phys. **2**, (1977) 115–119.

[7] M. Mezard, G. Parisi and M. A. Virasoro, *Spin Glass Theory and Beyond* (World Scientific, Singapore 1986);

[8] J.-S. Wang and R. H. Swendsen, Phys. Rev. B **37**, (1988) 7745.
(World Scientific, Singapore 1997).

[9] E. Marinari, G. Parisi, F. Ricci-Tersenghi, J. J. Ruiz-Lorenzo and F. Zuliani, J. Stat. Phys. **98** 973 (2000).

[10] A.J. Bray and M.A. Moore, in *Heidelberg colloquium on glassy dynamics*, edited by J.L van Hemmen and I. Morgenstern (Springer Verlag, Heidelberg, 1986); K.H. Fisher and J.A. Huse, Phys. Rev. Lett. **56**, (1986) 801 and Phys. Rev. B **38**, (1988) 386.

[11] R. Benzi and R. Petronzio, Europhys. Lett. **9**, (1989) 17–22.

[12] M.P. Nightingale, Physica **83A**, (1976), 561.

[13] M. Palassini and S. Caracciolo, Phys. Rev. Lett. **82**, (1999) 5128–5131

[14] H.G. Ballesteros, A. Cruz, L.A. Fernandez, V. Martin-Mayor, J. Pech, J.J. Ruiz-Lorenzo, A. Tarancon, P. Tellez, C.L. Ullod, C. Ungil Phys. Rev. B **62**, (2000) 14237.

[15] H. W. Blöte, L. N. Shchur and A. L. Talapov, Int. J. Mod. Phys. C **10**, 137 (1999).

[16] P.O. Mari and I.A. Campbell, cond-mat/0103619.

[17] M. Campostrini, A. Pelissetto, P. Rossi, E. Vicari, cond-mat/0201180 (2002).

[18] G. Parisi, R. Petronzio and F. Rosati, Eur. Phys. J. B **21**, (2001) 605–609; F. Rosati,Int. J. Mod. Phys. A **16**, (2001) 2111; F. Rosati, Ph.D. Thesis (2000).

[19] L. Gnesi, R. Petronzio and F. Rosati, in preparation